

Isolated Zirconium Chloride Clusters in the Phase $\text{Rb}_5\text{Zr}_6\text{Cl}_{18}\text{B}$. Generalities Regarding the Bonding, Stability, and Size of M_6X_{12} -Type Clusters with and without Interstitial Atoms

Robin P. Ziebarth and John D. Corbett*

Contribution from the Department of Chemistry, Iowa State University, Ames, Iowa 50011. Received August 18, 1988

Abstract: The cluster-phase $\text{Rb}_5(\text{Zr}_6\text{Cl}_{12}\text{B})\text{Cl}_6$ is obtained in high yield from reactions of Zr and B powders, RbCl , and a slight deficiency of ZrCl_4 in a sealed Ta container at 850 °C. The presence of isolated $\text{Zr}_6\text{Cl}_{18}\text{B}^{5-}$ clusters of $\sim D_{3d}$ symmetry was established by single-crystal X-ray diffraction means (space group $Pm\bar{3}n$; $Z = 2$; $a = 10.914$ (4) Å, $b = 9.078$ (4) Å, $c = 17.769$ (5) Å; $R, R_w = 2.5, 2.7\%$). Close-packed layers of clusters stack in an eclipsed manner to generate suitable chlorine polyhedra for three types of rubidium cations. The family of phases $\text{A}_x^1(\text{Zr}_6\text{Cl}_{12}\text{Z})\text{Cl}_n$ always contains interstitial Z within the clusters, and according to extended-Hückel MO results, the bonding is dominated by strong Zr-Z bonding and a t_{2g}^6 metal-metal bonding HOMO configuration. The predominance of 14-electron clusters in the chloride examples, the increased number of 15- and 16- e^- examples found in Zr_6I_{12} -type clusters, and the occurrence of only 15- and 16- e^- (Nb, Ta) $_6\text{X}_{12}$ -type clusters ($\text{X} = \text{Cl}, \text{Br}, \text{I}$) under normal synthetic conditions (but 14- and 15- e^- types for $\text{X} = \text{F}, \text{O}$) all correlate with the bonding character of the a_{2u} HOMO and matrix effects ($\text{X}^i\text{-X}^j$ repulsions) within the clusters. Larger repulsive distortions with large X, smaller M, or small Z all lead to decreased antibonding M-Xⁱ contributions in the a_{2u} HOMO and to 15- or 16- e^- clusters. The Zr-Z dimensions of all 14- e^- chloride clusters compare closely with those of the other ZrZ_x systems and show a regular decrease in the series $Z = \text{Be}, \text{B}, \text{C}$. Larger than expected dimensions are found for $Z = \text{N}$ or H where cluster size may instead be determined largely by Zr-Zr and Zr-Cl interactions. Electron-poorer clusters of Zr, Nb, and Ta can all be obtained near room temperature.

By far the most common cluster building block in transition-metal halides, if not in general, is the M_6X_{12} unit, an octahedron of metal atoms edge-bridged by inner halide X^i . An important feature of these clusters is that the exo or terminal positions at the six metal vertices are also strongly bonded to outer halide X^a (or other ligands). A series of cluster structure types with stoichiometries $(\text{M}_6\text{X}_{12})\text{X}_n$, $0 \leq n \leq 6$, can be generated via this functionality, the terminal positions being filled by some combination of X^i and X^a atoms. However, the breadth of the series that can be achieved is seriously limited in simple binary halide systems by the electronic bonding requirements of typical clusters; for example, $\text{Nb}_6\text{Cl}_{14}$ contains the only example of an $\text{Nb}_6\text{Cl}_{12}$ cluster in the system Nb-NbCl_5 .

The $(\text{M}_6\text{X}_{12})\text{X}_6$ terminal member of the stoichiometry series described above has been known in ternary niobium chlorides for some time.^{1,2} The representative $\text{K}_4\text{Nb}_6\text{Cl}_{18}$ ($=4\text{KCl}\cdot\text{Nb}_6\text{Cl}_{14}$) with 16 cluster-based electrons together with a variety of other $\text{Nb}_6\text{Cl}_{18}^{m-}$ ($m = 2, 3, 4$) salts prepared from it near room temperature have all been shown by single-crystal X-ray diffraction studies to contain isolated $(\text{Nb}_6\text{Cl}_{12})\text{Cl}_6^{m-}$ clusters.^{1,3,4} These one- and two-electron oxidations of the parent cluster produce systematic increases in the Nb-Nb distances, reflecting the removal of bonding electrons; however, only the $\text{Nb}_6\text{Cl}_{18}^{4-}$ example appears to be stable at high temperature. The significance of these compounds beyond their position at the end of the M_6X_{12} to M_6X_{18} cluster series is that they afford a facile route to a solution chemistry of $\text{Nb}_6\text{Cl}_{18}^{m-}$ clusters that is inaccessible in the solid state. Both reversible redox reactions of the clusters in solution and cluster insertion into clay systems that leads to pillared clays are examples of the chemistry now accessible.^{5,6}

Although $\text{Zr}_6\text{Cl}_{12}$ -type clusters exhibit similar structural features regarding inner Cl^i and outer vertex-bonded Cl^a atoms, a considerably greater versatility in Cl:M ratios can be achieved. This advantage accrues because all Zr_6X_{12} -type cluster examples appear to require the inclusion of an interstitial atom Z within in order to produce a cluster-based electron count that is at or near the preferred 14. (The range achieved so far in solid-state syntheses of all zirconium halides spans 13-16 e^- .) The additional variable provided by Z together with electronic changes produced when alkali-metal cations of different size and number are also incorporated in the structures generates a considerably larger family of cluster structures and compositions than possible heretofore. Known phases within the general family $\text{A}_x^1[\text{Zr}_6\text{Cl}_{12}(\text{Z})]\text{Cl}_n$ now encompasses $0 \leq n \leq 6$ and $0 \leq x \leq 6$. The range of n and of the structure types found for each are exemplified by $\text{Zr}_6\text{Cl}_{12}\text{H}_7$,⁷⁻⁹ $\text{KZr}_6\text{Cl}_{13}\text{Be}$,⁷ $\text{Zr}_6\text{Cl}_{14}\text{C}$,⁹ and $\text{KZr}_6\text{Cl}_{15}\text{Cl}^{10}$ plus analogues in three other structure types,¹¹⁻¹³ $\text{Na}_4\text{Zr}_6\text{Cl}_{16}\text{Be}$,¹⁴ and $\text{Ba}_2\text{Zr}_6\text{Cl}_{17}\text{B}$.¹³ We report here the first example of the $n = 6$ limit in which isolated $\text{Zr}_6\text{Cl}_{18}$ clusters are present.

A large body of information regarding this profusion of centered zirconium chloride cluster phases has been accumulated in the last few years. This is an appropriate time to provide some useful generalizations regarding particularly electronic, bonding, and dimensional properties that have not been considered before and that appear important in the stability of these compounds. In addition, the predominance of 14-electron cluster examples in the chlorides is in notable contrast to the number of electron-rich clusters found for the analogous zirconium iodides and, particularly, with the clear preference for 15- and 16-electron clusters in the longer known (and empty) $(\text{Nb}, \text{Ta})_6\text{X}_{12}$ -type cluster phases. Many of these observations can be correlated and interpreted in

(1) Simon, A.; von Schnering, H.-G.; Schäfer, H. *Z. Anorg. Allg. Chem.* **1968**, *361*, 235.

(2) Hughes, B. G.; Meyer, J. L.; Fleming, P. B.; McCarty, R. E. *Inorg. Chem.* **1970**, *9*, 1343.

(3) Wells, A. F. *Structural Inorganic Chemistry*; 5th ed.; Clarendon Press: Oxford, 1984; pp 432-437.

(4) Koknat, F. W.; McCarty, R. E. *Inorg. Chem.* **1974**, *13*, 295.

(5) Summarized by: Schäfer, H.; Plantz, H.; Baumann, H. *Z. Anorg. Allg. Chem.* **1973**, *401*, 63.

(6) Christiano, S. P.; Wang, J.; Pinnavaia, T. J. *Inorg. Chem.* **1985**, *24*, 1222.

(7) Ziebarth, R. P.; Corbett, J. D. *J. Am. Chem. Soc.* **1985**, *107*, 4572.

(8) Chu, P. J.; Ziebarth, R. P.; Corbett, J. D.; Gerstein, B. C. *J. Am. Chem. Soc.* **1988**, *110*, 5324.

(9) Ziebarth, R. P.; Corbett, J. D., accepted for publication in *J. Solid State Chem.*

(10) Ziebarth, R. P.; Corbett, J. D. *J. Am. Chem. Soc.* **1987**, *109*, 4844.

(11) Ziebarth, R. P.; Corbett, J. D. *J. Less-Common Met.* **1988**, *137*, 21.

(12) Ziebarth, R. P.; Corbett, J. D. *J. Am. Chem. Soc.* **1988**, *110*, 1132.

(13) Zhang, J.; Corbett, J. D., unpublished research.

(14) Ziebarth, R. P.; Corbett, J. D. *Inorg. Chem.* **1989**, *28*, 626.

Table I. Summary of Crystallographic and Refinement Data for $Rb_5Zr_6Cl_{18}B$

space group	<i>Pmna</i> (No. 53)
<i>Z</i>	2
<i>a</i> , Å	10.914 (4)
<i>b</i> , Å	9.078 (4)
<i>c</i> , Å	17.769 (5)
<i>V</i> , Å ³	1760 (1)
cryst dimens, mm	0.18 × 0.21 × 0.37
radiation	Mo $K\alpha$, graphite monochromator
2 θ (max), deg	55.0
scan mode	ω
octants	<i>hkl</i> ; $\bar{h}k\bar{l}$
no. of reflns	
measd	4528
obsd ^b	2750
indepndt	1437
<i>R</i> (av), %	1.5
μ , cm ⁻¹ (Mo $K\alpha$)	97.2
transm coeff range	0.74–1.00
secndry ext coeff	1.9 (3) × 10 ⁻⁶
<i>R</i> _c ^c %	2.5
<i>R</i> _w ^d %	2.7

^a From least-squares refinement of Guinier powder diffraction data with Si as an internal standard. ^b $F_o > 3\sigma_F$, $I_o > 3\sigma_I$. ^c $R = \sum ||F_o| - |F_c|| / \sum |F_o|$; $R_w = [\sum w(|F_o| - |F_c|)^2 / \sum w|F_o|^2]^{1/2}$, $w = 1/\sigma_F^2$.

terms of extended-Hückel MO results, especially (1) the role of the interstitial and of metal-metal bonding in the centered clusters and (2) the regular changes that occur in the stability of the a_{2u} HOMO for the 15th and 16th electron in M_6X_{12} units depending on the relative sizes of M and X, a so-called matrix effect. Finally, the collection of 18 structures determined for centered Zr_6Cl_{12} -type clusters provides good evidence for the reproducibility of and trends in effective sizes for the series of interstitials H, Be–N. Their effect in determining overall cluster dimensions also appears to influence the choice of structure for some stoichiometries.

Experimental Section

Synthesis. The sources of the materials, the synthetic methods utilizing welded Ta containers, and Guinier X-ray powder techniques have been recently described.¹⁰ The new phase $Rb_5Zr_6Cl_{18}B$ was initially obtained as the major product from the reaction of Zr powder, $ZrCl_4$, $RbCl$, and amorphous B powder at 850 °C proportioned for the hypothetical phase $Rb_4Zr_6Cl_{15}B$. The reaction was air-quenched after 13 days. The composition used was suggested by previous experiences in systems involving interstitial carbon atoms, where reactions loaded to prepare the hypothetical $M_3Zr_6Cl_{15}C$ ($M = Na, K, Rb$) had instead given products with powder diffraction patterns similar to that of $K_4Nb_6Cl_{18}$.¹ Electronically, an $M_4Zr_6Cl_{18}C$ composition seemed entirely plausible, simply the result of the reaction of the known phase $Zr_6Cl_{14}C$ with M^+Cl . Unfortunately, all of the carbide-cluster crystals examined were apparently twinned and structurally intractable, and attempts to index the X-ray powder patterns also failed. The $Rb_4Zr_6Cl_{15}B$ attempt, although failing to solve the problem with the $M_3Zr_6Cl_{15}$ -type carbides, provided a compound with an entirely new powder diffraction pattern, and the composition and structure were both established by single-crystal X-ray diffraction.

Subsequent experiments showed that $Rb_5Zr_6Cl_{18}B$ is most efficiently prepared by the reaction of Zr powder, $ZrCl_4$, $RbCl$, and amorphous B powder in amounts corresponding to the composition $Rb_5Zr_6Cl_{17}B$. The slightly reducing conditions appear to facilitate formation of the desired material, as was also observed earlier for $Cs_3Zr_6Cl_{16}Z$ ($Z = B, C$),¹⁴ while reactions loaded according to the stoichiometry $Rb_5Zr_6Cl_{18}B$ yielded an unidentified compound and Rb_2ZrCl_6 . Stoichiometric reactions for this new composition that were run with NaCl or KCl instead of $RbCl$ produced yet another unknown compound in the former case, and $K_2Zr_6Cl_{15}B$ ¹² and K_2ZrCl_6 in the latter.

As far as is known, the syntheses of these clusters are all under thermodynamic control. Thus, the composition loaded determines what is obtained, except for such features as temperature and the slight off-stoichiometry that favors the formation of the compound described here. For example, the preparation of $RbZr_6Cl_{14}B^9$ or $Rb_2Zr_6Cl_{15}B^{10}$ rather than $Rb_5Zr_6Cl_{18}B$ from $RbCl/ZrCl_4/Zr$ mixtures is largely determined by the relative amount of $RbCl$ used.

Crystallography. Diffraction data were collected at room temperature from a dark-red, rectangular prism of $Rb_5Zr_6Cl_{18}B$ by using ω -scans and monochromatic Mo $K\alpha$ radiation. The initial orthorhombic unit cell that

Table II. Positional Parameters for $Rb_5Zr_6Cl_{18}B$

atom	type	<i>x</i>	<i>y</i>	<i>z</i>	<i>B</i> _{iso} , Å ²
Zr1	4 <i>h</i>	0	0.14059 (7)	0.10858 (3)	1.76 (2)
Zr2	8 <i>i</i>	0.35076 (3)	0.15361 (5)	0.54965 (2)	1.71 (1)
Cl1	4 <i>e</i>	0.3321 (1)	0	0	2.39 (6)
Cl2	8 <i>i</i>	0.33388 (9)	0.0127 (1)	0.67368 (6)	2.50 (4)
Cl3	8 <i>i</i>	0.3327 (1)	0.3202 (1)	0.43381 (6)	2.64 (5)
Cl4	4 <i>h</i>	0	0.6679 (2)	0.11266 (9)	2.65 (7)
Cl5	8 <i>i</i>	0.3251 (1)	0.6825 (1)	0.11011 (7)	2.82 (5)
Cl6	4 <i>h</i>	0	0.2834 (2)	0.24198 (9)	2.99 (7)
Rb1 ^a	4 <i>h</i>	0	0.04118 (9)	0.66387 (4)	3.29 (3)
Rb2 ^b	4 <i>g</i>	1/4	0.47501 (9)	1/4	3.89 (4)
Rb3 ^c	4 <i>h</i>	0	0.4551 (3)	0.4801 (2)	7.6 (3)
B ^d	2 <i>a</i>	0	0	0	1.5 (2)

^a Occupancy refined to 0.997 (3). ^b Occupancy refined to 0.991 (4). ^c The other split position is $0, \bar{y}, \bar{z}$. The occupancy of each refined to 0.252 (2). ^d Occupancy refined to 1.05 (4).

was calculated from 12 tuned reflections first located by film methods¹⁵ was consistent with Polaroid axial photographs subsequently taken on the diffractometer in terms of both axial lengths and Laue symmetry. Details of the diffraction study are summarized in Table I.

The space group *Pmna* was chosen on the basis of the observed systematic extinctions and an assumption of centricity suggested by a Wilson plot. The phase solution was provided by MULTAN 80¹⁶ with the aid of two randomly oriented Zr_6 octahedra included as input to the normalization routine. Assignment of the two most intense peaks in a calculated Fourier map to zirconium atoms allowed the remaining atoms to be located in successive cycles of least-squares refinement and Fourier map calculations. The boron interstitial atom was found as an approximately five-electron residual in the cluster center on a difference map that was computed after absorption correction (ψ -scan) and isotropic refinement of all other atoms in the structure. Electron density maps calculated for the converged structure showed large streaks of positive density corresponding to maxima of four to five electrons running through the cell parallel to the \bar{a} and \bar{c} axes. This result was apparently a consequence of termination effects in the Fourier series, as difference Fourier maps were unaffected and showed residuals corresponding to less than ± 0.5 e⁻/Å³. This behavior presumably arises with the well-formed crystals that are often produced by transport reactions at high temperature.

The cations Rb1 and Rb2 gave normal refinements. However, the Rb3 atom initially positioned at $(0, 1/2, 1/2)$, a site of $2/m$ symmetry, exhibited an extremely long, cigarlike thermal ellipsoid in the approximately [011] direction with principal axial ratios of 1.5:14.7:1. The symmetry at the Rb3 site was accordingly reduced to *m* and the Rb3 atom allowed to move within the plane perpendicular to \bar{a} . Refinement of this split Rb3 site with equal occupancies proceeded smoothly to give two inversion-related atoms separated by 1.08 Å. Anisotropic thermal parameters of the disordered Rb3 atoms were more reasonable but still elongated, with principal axial ratios of 1.9:6.0:1. Additional reflections suggesting an ordered superstructure were not observed in any of the axial photographs taken on the diffractometer or in powder diffraction patterns of the compound. Attempts to reduce the space group symmetry to the acentric groups *Pmn*2₁ or *Pm*2₁ (the latter requires the origin be moved to $(1/4, 0, 1/4)$) exhibited coupling of pseudo-inversion-related parameters and failed to provide a more satisfactory fit of the data than the partially disordered *Pmna* model. Thermal parameters achieved for Rb3 were also 1.5–3.0 times larger in the long direction than those in the split atom, *Pmna* refinement. Further reductions in symmetry to monoclinic appeared to be unwarranted on the basis of the acentric orthorhombic refinements, the very satisfactory data averaging attained for *Pmna* ($R_{av} = 1.5\%$), the axial photographs, and the otherwise quite satisfactory refinement of the *Pmna* model with one disordered atom. The problem is similar to those encountered before when somewhat poorly suited cation sites are defined by a cluster anion network.^{10,12}

Application of a secondary extinction correction and a reweighting of the data in 10 overlapping groups sorted on $|F_{obsd}|$ to correct for underestimated errors for weak reflections gave final *R* and *R_w* values of 2.5 and 2.7%, respectively. The alternate refinement of the structure with the Rb3 atom constrained to the inversion center gave *R* and *R_w* values of 3.0 and 3.7%, respectively, strongly supporting the correctness of the split atom model.

(15) Jacobson, R. A. *J. Appl. Crystallogr.* 1976, 9, 115.

(16) Main, P.; Fiske, S. J.; Hull, S. E.; Lessinger, L.; Germain, G.; Declercq, J. P.; Woolfson, M. M. *MULTAN 80. A System of Computer Programs for the Automatic Solution of Crystal Structures from X-Ray Diffraction Data*; Department of Physics, University of York Printing Unit: York, England, 1980.

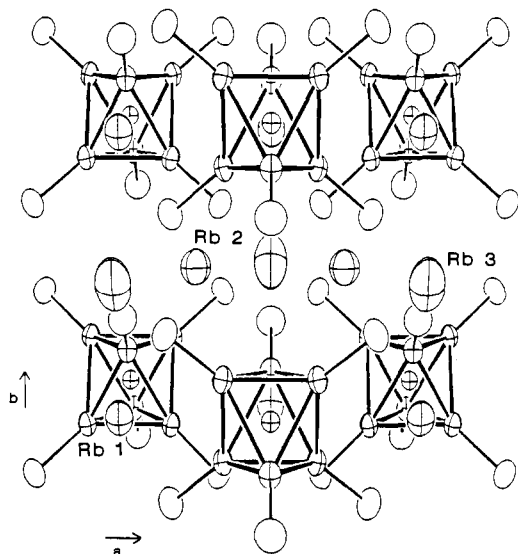


Figure 1. An approximately [001] view of the structure of $\text{Rb}_5\text{Zr}_6\text{Cl}_{18}\text{B}$ with Cl^{I} atoms omitted for clarity. Small crossed ellipsoids inside the trigonal antiprismatic Zr_6 clusters represent boron atoms. The Rb2 and Rb3 atoms lie between cluster layers, while Rb1 resides within the cluster layers (90% probability thermal ellipsoids).

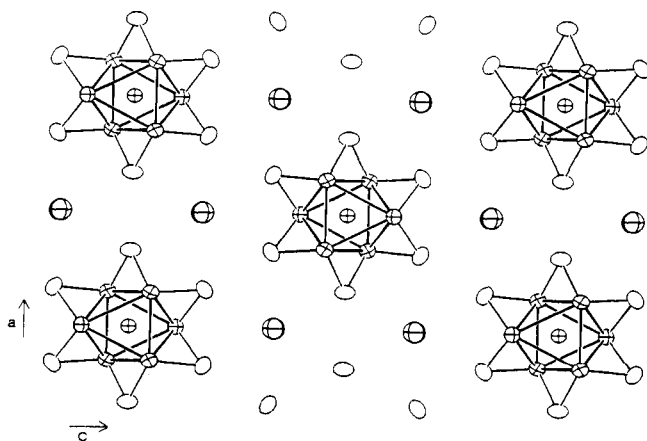


Figure 2. A [010] projection of the cluster columns in $\text{Rb}_5\text{Zr}_6\text{Cl}_{18}\text{B}$. The six Cl^{I} and the six Cl^{A} atoms that lie above and below each Zr_6B cluster have been omitted for clarity. Crossed ellipsoids between clusters are Rb1 atoms (50% ellipsoids).

Structural Results and Discussion of $\text{Rb}_5\text{Zr}_6\text{Cl}_{18}\text{B}$

Final positional parameters for $\text{Rb}_5\text{Zr}_6\text{Cl}_{18}\text{B}$ are given in Table II, and the important distances are compiled in Table III. Anisotropic thermal parameters as well as observed and calculated structure factor amplitudes are available as supplementary material.

The structure of $\text{Rb}_5\text{Zr}_6\text{Cl}_{18}\text{B}$ consists of isolated $[(\text{Zr}_6\text{Cl}_{12}\text{B})\text{Cl}_6]^{5-}$ clusters distributed in a sea of rubidium cations. The clusters occur in layers with the pseudo- $\bar{3}$ axis of each cluster oriented perpendicular to the cluster layers, as shown in Figure 1 in a view down the \bar{c} axis from which the Cl^{I} atoms have been omitted. Parallel to the \bar{b} axis the cluster layers stack directly on top of one another in an $\cdots\text{AA}\cdots$ manner to give columns of stacked $\text{Zr}_6\text{Cl}_{18}\text{B}^{5-}$ clusters. A projection of the cluster columns down \bar{b} in Figure 2 shows that the individual layers are approximately close-packed. The rubidium cations are distributed around the cluster columns, both within and between the cluster layers.

The individual $\text{Zr}_6\text{Cl}_{18}\text{B}$ clusters have crystallographically imposed $2/m$ (C_{2h}) symmetry with the mirror plane perpendicular to \bar{a} (Figure 1), but the Zr_6B units are observed to be mildly elongated along a pseudo- $\bar{3}$ axis parallel to \bar{b} . The Zr-Zr distances within the triangles normal to this nominal $\bar{3}$ axis are in fact all within 2σ of 3.254 Å, while distances of 3.299 (1) and 3.300 (1) Å between these give the metal cluster an apparent D_{3d} symmetry.

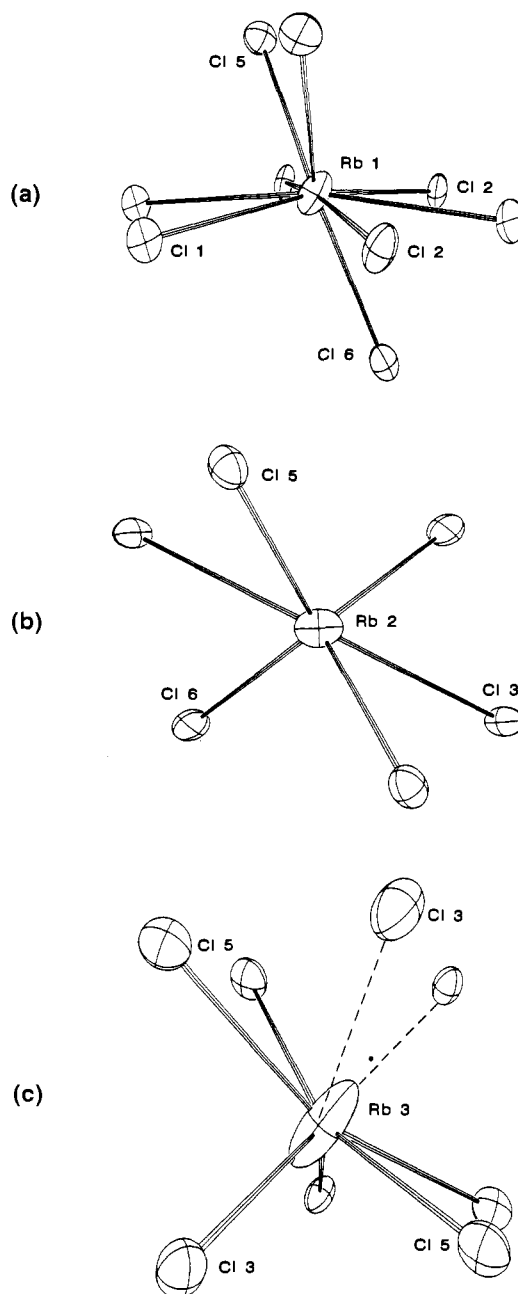


Figure 3. Rubidium cation sites in $\text{Rb}_5\text{Zr}_6\text{Cl}_{18}\text{B}$ (50% ellipsoids). (a) The nine-coordinate Rb1 site, which lies ~ 0.3 Å above the least-squares plane defined by the six Cl1 and Cl2 atoms shown. The Cl5 ($\times 2$) and Cl6 atoms above and below the plane are terminal Cl^{A} atoms. A crystallographic mirror plane lies approximately in the page. (b) The Rb2 site as viewed along the twofold axis; Cl5 and Cl6 are terminal atoms on the cluster. (c) The cavity about one of the quarter-occupied Rb3 positions. The other inversion-related site is indicated by the small filled circle. A mirror plane lies approximately in the page and an inversion center lies midway between the Rb3 positions. Dashed lines mark Rb3-Cl distances over 4.0 Å.

The Zr-B distances are consistent with a boron crystal radius of 1.46 Å which compares, for example, with 1.44 Å similarly deduced for the cluster $\text{Sc}_7\text{Cl}_{12}\text{B}$.¹⁷ These dimensional aspects will be generalized in a later section.

The rubidium atoms occupy three crystallographically distinct sites within the cluster anion array. These are illustrated in Figure 3. The Rb1 ion occupies a nine-coordinate site situated between clusters and within the cluster layer. As shown in Figure 3a, the site is bounded by a ring of six Cl^{I} atoms in a plane ~ 0.4 Å below the cation, plus two terminal Cl^{A} atoms above (Cl5) and one below

Table III. Interatomic Bonding Distances in $Rb_5Zr_6Cl_{18}B$ (Å)

Zr-Zr		Zr-Cl ^a	
Zr1-Zr2 (×4) ^a	3.2515 (9)	Zr1-Cl6 (×2)	2.702 (2)
Zr1-Zr2 (×4)	3.299 (1)	Zr2-Cl5 (×4)	2.655 (1)
Zr2-Zr2 (×2)	3.258 (1)		
Zr2-Zr2 (×2)	3.300 (1)	Rb-Cl	
\bar{d}	3.277	Rb1-Cl5 (×2)	3.294 (2)
		Rb1-Cl6 (×1)	3.388 (2)
		Rb1-Cl2 (×2)	3.418 (1)
Zr-B		Rb1-Cl1 (×2)	3.461 (1)
Zr1-B (×2)	2.3133 (8)	Rb1-Cl2 (×2)	3.657 (2)
Zr2-B (×4)	2.3186 (7)		
\bar{d}	2.3168	Rb2-Cl5 (×2)	3.225 (1)
		Rb2-Cl6 (×2)	3.239 (1)
		Rb2-Cl3 (×2)	3.668 (1)
Zr-Cl ^l		Rb3-Cl5 (×2)	3.237 (3)
Zr1-Cl3 (×4)	2.561 (1)	Rb3-Cl5 (×2)	3.247 (3)
Zr1-Cl2 (×4)	2.562 (1)	Rb3-Cl3 (×2)	3.920 (2)
Zr2-Cl2 (×4)	2.555 (1)	Rb3-Cl6 (×2)	4.509
Zr2-Cl4 (×4)	2.555 (1)		
Zr2-Cl3 (×4)	2.562 (1)		
Zr2-Cl1 (×4)	2.589 (1)		

^a Number of times the distance occurs per cluster or per cation.

(Cl6). The Rb-Cl distances range from 3.294 (2) to 3.657 (2) Å and average 3.450 Å. Summation of the crystal radii¹⁸ for chlorine and nine-coordinate rubidium gives 3.44 Å. The second rubidium resides in a six-coordinate site approximately midway between cluster layers that approximates a trigonal antiprism, Figure 3b. The rubidium atom lies distinctly closer to the rectangular face of the prism that is made up solely of terminal, and presumably more negative, chlorine atoms (Cl5, Cl6), 3.232 Å average, while the other two distances are 3.668 (1) Å, and the average is 3.377 Å. Both the Rb1 and Rb2 positions refined to full occupancy.

The last of the five cations, Rb3, is located midway between cluster layers within a somewhat oversized eight-coordinate site of $2/m$ symmetry, Figure 3c. The central position at the inversion center would place rubidium coplanar with four Cl5^a atoms at 3.196 Å and much more distant, 4.151 Å, from four Cl3 atoms, two above and two below. The actual situation appears similar to that found for cations in other cluster matrices;^{10,12} the rubidium refines as two positions that are each one-fourth occupied and displaced from the midpoint by ± 0.54 Å toward a pair of the more distance Cl3 atoms. This displacement reduces distances to each of the Cl3 atoms by 0.22 Å while lengthening the separation from each of four Cl5^a atoms by only 0.04 Å. The average Rb3-Cl distance in the six-coordinate site is 3.468 Å. This is clearly the least favorable cation site, and the refinement parameters reflect a necessary compromise for bonding of Rb3. The overall half-occupancy of the combined sites is dictated by the electronic requirements of the cluster (below).

The eclipsed stacking of clusters in $Rb_5Zr_6Cl_{18}B$, Figure 2, appears to be a favorable cluster arrangement for generating three types of approximately equal-sized cation sites per cluster while maximizing the number of rubidium contacts to the presumably more negative terminal chlorine atoms. The columnar stacking provides an average of 3.6 Cl^a neighbors to each rubidium, three for the two Rb1 ions and four each for two Rb2 and one Rb3. In contrast, the $K_4Nb_6Cl_{18}$ structure,¹ which contains only four cation sites per cluster and hence cannot be used for $Rb_5Zr_6Cl_{18}B$, affords just three terminal chlorine atom contacts per cation. The nearly close packed clusters in the recently discovered $Li_6Zr_6Cl_{18}H^{19}$ have six equivalent, six-coordinate sites per cluster for the smaller cations, but these also allow only three Cl^a contacts per cation.

The structure of $Rb_5Zr_6Cl_{18}B$ may also be viewed in terms of close-packed chlorine layers stacked normal to \bar{b} with an ordered

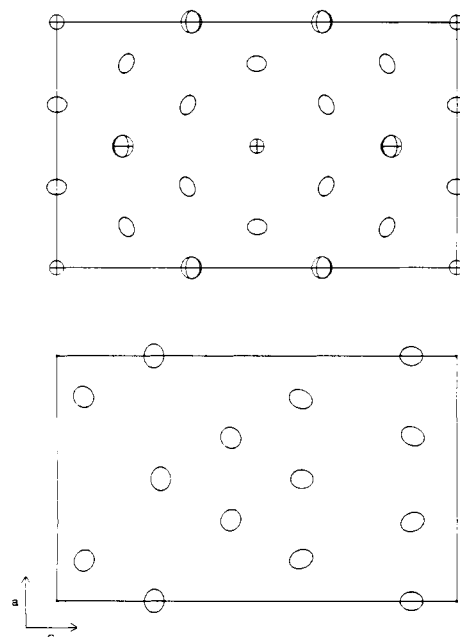


Figure 4. Layered description of $Rb_5Zr_6Cl_{18}B$. Top: A [010] projection on $y = 0$ of the close-packed layer of atoms designated A. The large and small crossed ellipses represent Rb1 and B atoms, respectively, while open ellipses are Cl^a atoms. Bottom: A [010] projection on $y = 1/3$ of the layer of chlorine atoms denoted B'. The triangular zone of close-packed chlorine atoms in the center of the figure is related to others by a twofold axis normal to the projection plane at $(1/4, y, 1/4)$. Terminal chlorine atoms occupy the vertices of the triangular zones.

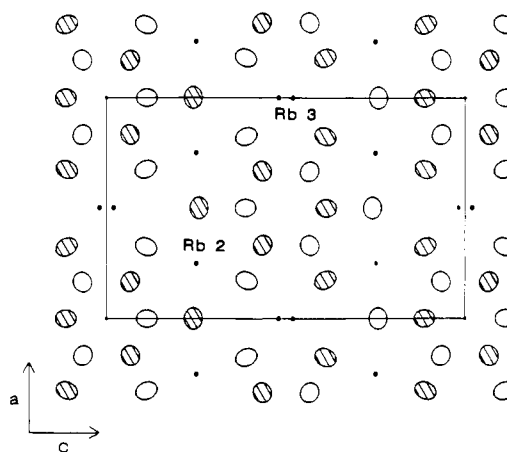


Figure 5. A [010] projection of the B' (open ellipses at $y = 1/3$) and B'' (striped ellipses, $y = 2/3$) layers in $Rb_5Zr_6Cl_{18}B$. The Rb2 and Rb3 cation sites near $y = 1/2$ are marked with isolated and paired solid circles, respectively. Note the unoccupied trigonal antiprismatic sites at the corner and center of the section near $y = 1/2$ that are bounded only by Cl^a atoms.

arrangement of zirconium atoms in Cl₅B octahedra between the layers. The top of Figure 4 shows the layer termed A at $y = 0$ that runs through the center of the cluster layer and is made up of a close-packed array of 12 chlorine, 2 boron, and 4 Rb1 atoms per cell. The second B' layer below at $y \approx 1/3$ is a pseudo-close-packed layer made up of zones of six close-packed chlorine atoms separated by narrow gaps. This layer is similar in nature to the B' layer in $K_2Zr_6Cl_{15}B^{12}$, and as before, the triangular zones correspond to regions of B- and C-type packing in a cubic-close-packed system. The narrow gaps are necessary to maintain minimal Cl-Cl distances. Finally, the third layer, B'' at $y \approx 2/3$, is related to B' by an inversion through $(1/2, 1/2, 1/2)$ (or an n -glide normal to \bar{b}).

The layer stacking in $Rb_5Zr_6Cl_{18}B$ is then described as ... AB'B''... with zirconium atoms occupying all the trigonal antiprismatic sites between the A and B' and A and B'' layers, that

(18) Shannon, R. D. *Acta Crystallogr., Sect. A* 1976, A32, 751.

(19) Ziebarth, R. P.; Zhang, J.; Corbett, J. D., to be submitted for publication.

is, those that surround the boron atoms in A. Rubidium cations are found both in the A layer (Rb1, Figure 4a) and between the B' and B'' layers. A projection of the B' and B'' layers and the Rb2 and Rb3 sites between them is shown in Figure 5. Interestingly, a potential site for another cation exists at the corners and center of this section (site type $2d$) as a small octahedral hole between clusters along b , i.e., within the cluster columns. Distances from the center of this site to the neighboring chlorine atoms are 2.727 ($\times 4$) and 2.516 ($\times 2$) Å, suggesting a lithium cation (\sum crystal radii = 2.57 Å) might be accommodated in a phase like $\text{LiRb}_5\text{Zr}_6\text{Cl}_{18}\text{Be}$ or $\text{LiK}_5\text{Zr}_6\text{Cl}_{18}\text{Be}$.

Structurally, $\text{Rb}_5\text{Zr}_6\text{Cl}_{18}\text{B}$ can easily be derived from that of $\text{Cs}_3\text{Zr}_6\text{Cl}_{16}\text{C}$, which is $\text{Cs}_3(\text{Zr}_6\text{Cl}_{12}\text{C})\text{Cl}_4^{2-}$,⁹ through the addition of 2 mol of M^1Cl per cluster to open the remaining $\text{Cl}^{\text{a-a}}$ bridges while retaining the spatial arrangement and orientation of the clusters within the layer. The structure of $\text{K}_4\text{Nb}_6\text{Cl}_{18}$ ¹ also shows a close relationship to that of $\text{Rb}_5\text{Zr}_6\text{Cl}_{18}\text{B}$. The former is also built-up of close-packed layers of clusters, in this case coincident with the [001] plane, but the stacking of the cluster layers is staggered because of the pseudotranslation provided by the 115° monoclinic angle. In addition, while the orientation of every cluster within a layer in $\text{K}_4\text{Nb}_6\text{Cl}_{18}$ is identical, the cluster centered on the [010] face of $\text{Rb}_5\text{Zr}_6\text{Cl}_{18}\text{B}$, Figure 2, is related to those on the cell corners by a twofold rotation axis.

Comparisons of Cluster Structure and Stability

Several dozen zirconium cluster compounds have been synthesized and studied in the few years since the importance, indeed the necessity, of the interstitial element within the clusters was first recognized.^{7,20} The character of these compounds subdivide surprisingly well into two contrasting families with respect to structures, stoichiometries, and the range of interstitials possible, namely, the chlorides and the iodides. The accumulated information on these clusters has to date not received any systematic consideration regarding the bonding, especially the effects of Z and halide on electronic structure and cluster (phase) stability and the relationship of these examples to the empty halide clusters known for niobium and tantalum. The combined effects of the sizes of metal, halide, and interstitial, if any, appear to produce significant regularities regarding the most stable electron counts for the entire group of clusters.

A considerable versatility among zirconium chloride cluster phases can be achieved by controlled manipulation of three variables in the $\text{A}_x^1(\text{Zr}_6\text{Cl}_{12}\text{Z})\text{X}_n$ family, namely, the values of x and n along with the valence electron count of the interstitial Z. In addition, a complement of 14 cluster-based electrons is clearly favored when Z is a main-group element (below), so much so that the syntheses of certain stoichiometries and structures can often be "driven" by the choice of Z and the proportions of the reactants. To date only H and Be-N have been incorporated as a main-group Z in zirconium chlorides. The Z examples from the second period in all cases refine to substantially full occupancy, and no cluster phase has been synthesized under equilibrium (high-temperature) conditions that appears to lack an interstitial atom. As a corollary, ZrCl_4 -Zr reactions run without a suitable Z element will provide primarily ZrCl_x compounds, $1 \leq x \leq 3$, with the distribution dependent mainly on the Zr:Cl ratio in the reactants.

Structure and Bonding in Zirconium Chloride Clusters. A good understanding of the role of the interstitial atom in the bonding and stabilization of $\text{Zr}_6\text{Cl}_{12}$ -type clusters can be obtained from the results of extended-Hückel molecular orbital calculations. Several authors have previously examined the bonding in isolated and empty $\text{Nb}_6\text{X}_{12}^{n+}$ clusters,²¹⁻²³ and although their results predict the right number of metal-metal bonding orbitals, these are in

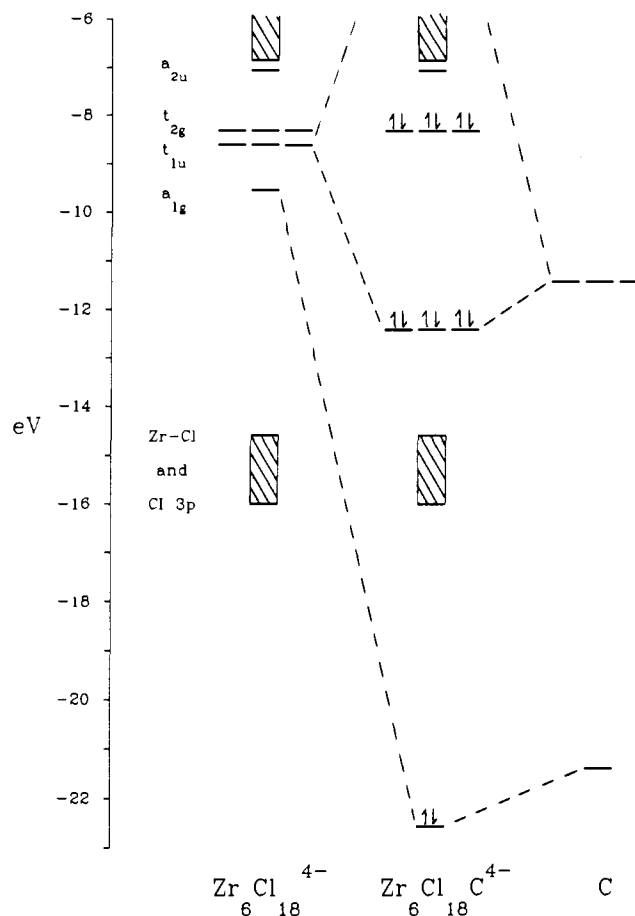


Figure 6. Cluster molecular orbital diagram from extended-Hückel calculations. Left: The hypothetical $\text{Zr}_6\text{Cl}_{18}^{4-}$ cluster (O_h); right: atomic carbon; center: the centered $\text{Zr}_6\text{Cl}_{18}\text{C}^{4-}$ cluster (O_h).

error because of the failure to include evidently indispensable terminal halogens (or other ligands) in the calculations. The importance of these exo groups in correctly establishing the symmetries and energy ordering of the metal-metal bonding levels for the cluster has been discussed in detail in connection with earlier calculations on zirconium iodide clusters with and without interstitial atoms.^{20,24} Obviously, inclusion of the terminal bonding interactions in the calculations on centered clusters seems particularly vital since the Zr-X^a interactions will transform the same as the opposed Zr-Z bonding. At the same time, the results of suitably formulated calculations on $\text{Zr}_6\text{I}_{12}\text{Z}$ clusters are not completely suitable for the zirconium chlorides since their cluster chemistries appear to be distinctly different. The larger iodine atoms produce more severe cluster distortions (matrix effects; see below), which are probably a major reason why the iodide clusters are much more accommodating of larger main-group Z elements from the third and fourth periods. In addition, the structural versatility that has been achieved to date with the iodides is much smaller, the known structure types being limited to only two, the Zr_6I_{12} and $(\text{A}^1)\text{Zr}_6\text{I}_{14}$ compositions.^{20,24-26}

In the course of this work, calculations have been carried out for the hypothetical empty cluster $(\text{Zr}_6\text{Cl}_{12})\text{Cl}_6$ with several sizes and for $(\text{Zr}_6\text{Cl}_{12}\text{Z})\text{Cl}_6$ models containing a variety of interstitials. As these differ only in details regarding overlap and energy parameters, the results for a carbide example will be described first and then compared with those for a beryllide with respect to overlap populations, charge transfer, and metal-metal bonding. Molecular geometries and parameters used to describe the atomic orbital energies and spatial characteristics are given in the supplementary material.²⁷

(20) Smith, J. D.; Corbett, J. D. *J. Am. Chem. Soc.* **1985**, *107*, 5704.

(21) Cotton, F. A.; Haas, T. E. *Inorg. Chem.* **1964**, *3*, 10.

(22) Robbins, D. J.; Thomson, A. J. *J. Chem. Soc., Dalton Trans.* **1972**, 2350.

(23) Bursten, B. E.; Cotton, F. A.; Stanley, G. G. *Isr. J. Chem.* **1980**, *19*, 132.

(24) Smith, J. D.; Corbett, J. D. *J. Am. Chem. Soc.* **1986**, *108*, 1927.

(25) Smith, J. D.; Corbett, J. D. *J. Am. Chem. Soc.* **1984**, *106*, 4618.

(26) Rosenthal, G.; Corbett, J. D. *Inorg. Chem.* **1988**, *27*, 53.

The one-electron molecular orbital energies for a hypothetical, unoccupied $Zr_6Cl_{18}^{4-}$ cluster are shown on the left side of Figure 6. A block of 18 chlorine 3s orbitals centered at -30.5 eV are off the bottom of the figure. The 54 molecular orbitals that are associated with Zr–Cl bonding and chlorine 3p lone pairs fall in a group between -16.0 and -14.5 eV. Considerable mixing between the Zr–Cl bonding orbitals and chlorine lone pairs prevents separation of the two groups. These $18 + 54 = 72$ filled orbitals represent all of the chlorine 3s and 3p valence levels. The next eight orbitals are principally metal-based and cluster bonding orbitals that are responsible for the metal–metal bonding, viz., a_{1g} , t_{1u} , t_{2g} , and a_{2u} in order of increasing energy. Above these lie sets of metal–metal and metal–chlorine antibonding levels. The size of the ~ 1.4 -eV gap between the seventh (t_{2g}) and eighth (a_{2u}) cluster orbitals is partially a consequence of an antibonding Zr–Cl component in the a_{2u} orbital. The hypothetical $Zr_6Cl_{18}^{4-}$ cluster with $(6 \times 4) - (18 \times 1) + 4 = 10$ cluster electrons and an $(a_{1g})^2(t_{1u})^6(t_{2g})^2$ configuration clearly can contain at least four more bonding electrons and needs six more to fill all of the metal–metal bonding states.

The effect of the interstitial carbon atom in stabilizing the $Zr_6Cl_{18}^{4-}$ cluster is depicted in the remainder of Figure 6. Two things will be noticed immediately: (1) there is a strong interaction between the carbon orbitals and the symmetry-equivalent cluster orbitals, and (2) the number of cluster bonding orbitals does not change, only their energies. The molecular orbital diagram for the centered cluster $Zr_6Cl_{18}C^{4-}$ is much the same as that of the unoccupied unit of the same dimensions except for two significant changes in the metal–metal bonding region. Interaction of the carbon 2s orbital with the lowest energy Zr–Zr bonding orbital (both of a_{1g} symmetry) creates a low-lying a_{1g} orbital at -22.6 eV, primarily carbon in character although a small zirconium contribution is discernible, and a t_{1u} set of Zr–C bonding orbitals is formed in a similar manner at -12.4 eV. In both instances, the antibonding combinations of carbon and cluster orbitals are at high energy and lie off-scale; thus, the total number of cluster bonding orbitals remains unchanged at eight on inclusion of the interstitial atom.

There appears to be no zirconium halide cluster phase that does not contain an interstitial atom, and all known reduced compounds containing Zr, Cl, and C can be described in terms of clusters or condensed clusters. In terms of Figure 6, the pronounced stabilization of the cluster by the interstitial atom can be attributed both to the formation of strong Zr–interstitial bonds and to the addition of the interstitial atom's valence electrons to the cluster bonding manifold. For electron counting purposes, the interstitial atom's valence electrons are "donated" to the cluster because no change in the number of cluster bonding orbitals has occurred, so that $Zr_6Cl_{18}C^{4-}$ has an $(a_{1g})^2(t_{1u})^6(t_{2g})^6$ configuration. However, this conventional electron counting procedure definitely does not imply a charge transfer from the interstitial atom to the metal cluster. Rather the bonding is largely covalent, with the four bonding orbitals in the carbide example having somewhat more carbon than zirconium character. The charge on carbon is calculated to be about -1.8 , and although the magnitude of the charge transfer is probably exaggerated, it is certainly correct in sign. For comparison, a carbon charge of the order of -0.5 to -1.0 has been estimated from detailed band calculations on the conceivably less polar ZrC (NaCl type).²⁸ XPS data for the carbon 1s core in the zirconium chlorides also support the charge transfer to carbon, there being a sizable shift to lower binding energies from 285.0 eV for the adventitious (hydro)carbon reference to 282.0 eV in $Zr_6Cl_{14}C$ and 282.8 eV in the related, condensed cluster-phase Zr_2Cl_2C .²⁹

(27) Although virtually all of the structurally well-defined $Zr_6Cl_{12}Z$ -type clusters are distorted from O_h symmetry, all calculations were for the sake of simplicity done on idealized octahedral clusters with suitably averaged observed dimensions. The major effect of the distortions is simply to remove the orbital degeneracies imposed by the higher symmetry, but the splittings are all quite small (<0.2 eV) and do not change either the ordering of any cluster orbitals or any conclusions.

(28) Neckel, A. *Int. J. Quantum Chem.* **1983**, *23*, 1317.

Table IV. Metal–Metal Overlap Populations and Bonding for Isoelectronic $Zr_6Cl_{18}Z^{n-}$ Clusters of Fixed Dimensions

orbital	cluster		
	$Zr_6Cl_{18}^{8-}$	$Zr_6Cl_{18}C^{4-}$	$Zr_6Cl_{18}Be^{6-}$
Σ Zr–Zr Overlap Populations			
a_{1g}	0.994	0.058	0.262
t_{1u} ($\times 3$)	0.562	0.070	0.317
t_{2g} ($\times 3$)	0.347	0.347	0.347
total	3.721	1.309	2.254
% Zr–Zr Bonding Retained ^a			
a_{1g}		6	26
t_{1u}		12.5	56.5
t_{2g}		100	100
total		35	61

^a 100Σ Zr–Zr overlap population of $Zr_6Cl_{18}Z^{n-} / \Sigma$ Zr–Zr overlap population of $Zr_6Cl_{18}^{8-}$.

The rather straightforward MO description of these clusters does not suggest there is anything particularly unusual about the bonding in these units. Although there are seven electron pairs in the neighborhood of the interstitial atom, symmetry alone requires that only four of these are actually involved in bonding to the s and p valence orbitals of a main-group interstitial atom. *Hypervalency* descriptors for these centered clusters therefore seem unnatural and unnecessary. The presence of six rather than four zirconium neighbors about carbon or boron (or hydrogen!) in the cluster is an obvious way in which a metal-rich network can retain some metal–metal bonding while at the same time forming strong polar metal–nonmetal bonds. The same is true in many extended solids even when simple valence rules are met, as in ZrC where the six-coordination of each atom in an NaCl-type structure is an obvious consequence of atom sizes and the same strong heteroatomic bonding.³⁰ The double-metal-layered Zr_2Cl_2C represents an interesting intermediate degree of cluster condensation in which carbon still has an "octahedral" environment, and an extended-Hückel description of the surprisingly localized Zr–C bonding therein differs from that in the $Zr_6Cl_{18}C^{4-}$ cluster only in small detail, not in kind.³¹

Metal–Metal Bonding. Although the strength of the metal–interstitial bonding is a major factor in stabilizing the metal framework of the centered zirconium clusters, significant amounts of metal–metal bonding also remain, and this appears to be important in cluster formation and stability, particularly in compounds with the less electronegative interstitial elements. Six electrons in 14-electron centered clusters are exclusively involved for metal–metal bonding (t_{2g}^6), although the magnitude is obviously dependent on the effective interstitial size. However, it should be noted that appreciable Zr–Zr overlap is contained in the metal–interstitial bonding MOs as well. Comparison of metal–metal overlap populations summed over the occupied cluster orbitals provides a good assessment of the differences in metal–metal bonding between centered and empty clusters of the same size and between clusters with different interstitial atoms. As shown in Table IV, the centered cluster $Zr_6Cl_{18}C^{4-}$, for instance, retains only 35% of the metal–metal bonding of the empty and isoelectronic cluster $Zr_6Cl_{18}^{8-}$. Approximately 80% of the Zr–Zr bonding in the centered cluster comes from the t_{2g}^6 set, while the remaining 20% comes from metal–metal overlap in the a_{1g} and t_{1u} MOs that are principally Zr–C bonding. In other words, the latter orbitals retain only about 6 and 12.5% of their Zr–Zr bonding character, respectively, on carbon inclusion.

On the other hand, the relative energies of the interstitial atom's valence orbitals strongly influence the percentage of interstitial character in these a_{1g} and t_{1u} molecular orbitals and, hence, the

(29) Hwu, S.-J.; Ziebarth, R. P.; Winbush, S. v.; Ford, J. E.; Corbett, J. D. *Inorg. Chem.* **1986**, *25*, 283.

(30) Wijeyesekera, S. D.; Hoffman, R. *Organometallics* **1984**, *3*, 949.

(31) Ziebarth, R. P.; Hwu, S.-J.; Corbett, J. D. *J. Am. Chem. Soc.* **1986**, *108*, 2594.

degree of metal-metal bonding that is retained. For instance, the valence orbital ionization energies of the beryllium 2s and 2p orbitals lie at -10.0 and -6.0 eV, respectively, well above the respective carbon values of -21.4 and -11.4 eV. As a result, there is significantly more zirconium mixing into the a_{1g} and t_{1u} sets, and the beryllium-centered cluster is calculated to retain more than 60% of the Zr-Zr bonding present in the isoelectronic but unoccupied cluster. In detail, the a_{1g} and t_{1u} orbitals are found to retain 26 and 56.5%, respectively, of the Zr-Zr bonding character of the equivalent orbitals in the unoccupied cluster (Table IV). The smaller beryllium contribution to these same orbitals now produces a calculated charge of -0.2 on the interstitial atom. Of course, the absolute magnitudes of these bonding effects will be somewhat different in real clusters since the beryllium entity is larger than that containing carbon, as will be considered in a later section.

Preferred Electronic Configurations. The importance of the 14-electron configuration indicated by the last figure is supported by numerous synthetic results, including those of many experiments particularly designed to test the configurational boundaries. Only a few 13- and 15-electron examples have been found among the 35-plus zirconium chloride cluster phases of known structure and stoichiometry that contain a main-group element. Three of the five 13-electron examples are hydrides, $Zr_6Cl_{12}H$, $Li_6Zr_6Cl_{18}H$, and $Ml_2ZrCl_6 \cdot Zr_6Cl_{12}H$.^{9,19,32} These may represent a "something is better than nothing" bonding mode; the clusters are oversized for hydride (see below), and the interstitial is evidently "rattling".⁸ The other two 13-e⁻ exceptions are $K_2Zr_6Cl_{15}Be^{12}$ and $Zr_6Cl_{14}B$.⁹ Only two 15-electron clusters with a clearly occupied a_{2u} level are known, $Cs_3Zr_6Cl_{16}C^{14}$ and $KZr_6Cl_{15}N$.¹⁰ The fact that the last two occur with relatively small interstitials will be seen to present a consistent trend.

The ubiquity of 14-electron zirconium chloride clusters when these contain main-group elements and the ease of their formation compared with 15- and 16-electron possibilities at first appear a little anomalous in light of the calculations represented in Figure 6, which clearly suggest a limit of 16 electrons in eight metal-metal bonding orbitals. The theoretical result is in fact more consonant with the greater number of 15- and 16-electron clusters known both for analogous zirconium iodides^{20,24,26} and binary and ternary niobium and tantalum halides,^{1,3,33-37} as well as with the regular decrease in metal-metal distances observed in a series of 14-, 15-, and 16-electron $Nb_6Cl_{18}^{m-}$ clusters.⁴ Before an interpretation is provided for these differences, it must be remembered that "stability" or its absence is not an absolute quantity but instead represents a relationship with alternate phases, and these may not be the same in all cases. Overreduction of zirconium chloride clusters leads to $Zr_2Cl_2Z^{29}$, whereas phases containing the 15- or 16-electron $(Nb,Ta)_6(Cl,Br)_{12}$ -type units as well as the lowest zirconium iodide $Zr_6I_{12}C$, etc., are in equilibrium with the respective metal (and ZrC, etc.) under the usual high-temperature synthetic conditions. Nonetheless, there are also some dimensional and angular differences in all these clusters that clearly parallel, and perhaps "explain", the stability trends noted above.

Matrix Effects and Interstitial Bonding. The dimensions observed for a M_6X_{12} -type cluster often represent a compromise between M-M and M-X bonding attractions and $X \cdots X$ closed-shell repulsions. This example of a matrix effect³⁸ is often seen in the degree to which each vertex of the metal octahedral unit is pulled inside the plane defined by the four adjoining X^i atoms, or the halides are forced outward. This deviation and thence the matrix effect would be expected to be greater for small M, large

X or, when relevant, small Z. In the case of an extreme difference, the M_6X_{12} cluster evidently becomes unstable with respect to the electron-richer M_6X_8 (face-capped) cluster alternative, as found in $(Nb_6I_8)I_{6/2}$ and $Mo_6X_8X_4$.

Two bonding factors appear to be important in the 14-electron preference shown by centered zirconium chloride clusters. The first relates to the matrix effect. Compared with zirconium iodide clusters, the magnitude of the $Zr(xy)-X^i$ antibonding (π^*) contribution to the Zr-Zr bonding a_{2u} MO, which would contain the 15th and 16th electrons, is larger in the zirconium chlorides since the $M-X^i_4$ cluster faces come closer to planarity. The difference in percentage of X^i character in the a_{2u} orbital, 10.3 and 8.0% for the $Zr_6Cl_{18}^{4-}$ and $Zr_6I_{18}^{4-}$, respectively, at typical cluster dimensions has somewhat complex origins, being a consequence of the greater Zr-I separations, the more diffuse 5p orbitals on iodine, and a smaller Zr-Iⁱ overlap in this representation owing to greater cluster distortion. A useful measure of this last matrix effect, and hence changes in the overlap, is the trans X^i-Zr-X^i angle across corners of the square of X^i atoms around each zirconium vertex. The larger the matrix effect, the smaller the angle, and the poorer the overlap. These angles range from 156 to 163° in the zirconium iodide carbide clusters²⁰ and from 167 to 171° in the zirconium chloride carbides.

A further implication is that 15- and 16-electron zirconium clusters should form more easily in systems in which smaller interstitial atoms produce a smaller M_6 unit, a larger matrix effect, and thence smaller antibonding contributions to $a_{2u}(xy)$. Indeed, $KZr_6Cl_{15}N$ (15 e⁻, $KZr_6Cl_{15}C$ type)¹⁰ represents the first example prepared under this reasoning. Of course, such deviations should be more frequent with the zirconium iodides, and $CsZr_6I_{14}C$ (15 e⁻) and $Zr_6I_{12}C$ (16 e⁻) are dominant in the carbon system.²⁰ A parallel between more reduced clusters and larger matrix effects also extends to the empty $(Nb,Ta)_6X_{12}$ clusters.

The absence of an interstitial and the smaller niobium provide $\bar{d}(Nb-Nb)$ distances in the chlorides that are between 0.2 and 0.4 Å less than analogous $\bar{d}(Zr-Zr)$ (3.20-3.30 Å),^{33,34} and as a result, the few trans $Cl^i-Nb-Cl^i$ angles that have been well determined lie between 161 and 167°^{4,39} comparable to those in the zirconium iodides. A parallel matrix effect and the concomitant lessening of M-Xⁱ antibonding contributions to a_{2u} are again consistent with the formation of only 15- and 16-e⁻ cluster halides of the group 5 metals under equilibrium conditions. Thus, just 16-e⁻ clusters in $Nb_6Cl_{14}^{33}$ are thermodynamically stable in the chloride system. In fact, high-temperature reactions in binary niobium chloride, bromide, and iodide systems with 14 available electrons per six metal atoms, i.e., those with a Nb:X ratio of 6:16, preferentially provide the trimeric cluster phases Nb_3X_8 ^{40,41} instead of Nb_6X_{16} cluster compositions, while ternary reactions aimed at 15-electron units yield instead the tetrameric $(Cs,Rb)Nb_4Cl_{11}$ with the same electron count per metal atom.⁴²

On the other hand, a 15-e⁻ example occurs, naturally enough, as the fluoride Nb_6F_{15} .³⁴ The greatly lessened matrix effects with the smaller fluoride are manifested by Nb-Nb distances of 2.80 Å compared with 2.915 Å in $Nb_6Cl_{18}^{4-}$. Interestingly, comparable Nb-Nb distances, 2.80-2.83 Å, have recently been found in Nb_6O_{12} -type clusters in $Mg_3Nb_6O_{11}$ (14 e⁻),⁴³ $Na_3Al_2Nb_3O_{64}$ (15 e⁻),⁴⁴ and $SrNb_6O_{14}$ (14 e⁻).⁴⁵ The electron counts are clearly in the right direction relative to that in the chloride, although the higher anion field and more complex nonmetal sharing necessary with oxygen in most cases might mean that close parallels with halide should not be expected. Tantalum cluster halides obtained under equilibrium conditions are comparably or slightly less re-

(32) Imoto, H.; Corbett, J. D.; Cisar, A. *Inorg. Chem.* **1981**, *20*, 145.(33) Simon, A.; Schnering, H.-G.; Wöhrle, H.; Schäfer, H. *Z. Anorg. Allg. Chem.* **1965**, *339*, 155.(34) Schäfer, H.; Schnering, H.-G.; Niehues, K.-J. *Nieder-Vahrenholz, H. G. J. Less-Common Met.* **1965**, *9*, 95.(35) McCarley, R. E.; Boatman, J. C. *Inorg. Chem.* **1965**, *4*, 1486.(36) Bauer, D.; Schnering, H.-G.; Schäfer, H. *J. Less-Common Met.* **1965**, *8*, 388.(37) Bauer, D.; von Schnering, H.-G. *Z. Anorg. Allg. Chem.* **1968**, *361*, 259.(38) Corbett, J. D. *J. Solid State Chem.* **1981**, *37*, 335; *39*, 56.(39) Koknat, F. W.; McCarley, R. E. *Inorg. Chem.* **1972**, *11*, 812.(40) von Schnering, H.-G.; Wöhrle, H.; Schäfer, H. *Naturwissenschaften* **1961**, *48*, 159.(41) Simon, A.; von Schnering, H.-G. *J. Less-Common Met.* **1966**, *11*, 31.(42) Broll, A.; Simon, A.; von Schnering, H.-G.; Schäfer, H. *Z. Anorg. Allg. Chem.* **1969**, *367*, 1.(43) Burnus, R.; Köhler, J.; Simon, A. *Z. Naturforsch.* **1987**, *42B*, 536.(44) Köhler, J.; Simon, A. *Angew. Chem., Int. Ed. Engl.* **1986**, *25*, 996; *Z. Anorg. Allg. Chem.* **1987**, *553*, 106.(45) Köhler, J.; Simon, A.; Hibble, S. J.; Cheetham, A. K. *J. Less-Common Met.* **1988**, *142*, 123.

duced than with niobium, viz., Ta_6X_{14} , $X = Br, I$,^{35,36} and Ta_6X_{15} , $X = Cl, Br, I$.³⁷

The second factor, and clearly important in zirconium cluster stability relative to that for analogous niobium and tantalum halides, is the strength of the additional Zr–Z bonding. The stabilizing influence of the interstitial atom is particularly evident in the number of $Zr_6X_{12}Z$ clusters listed above that have been prepared with fewer than 14-cluster bonding electrons, which is the apparent lower limit for the interstitial-free $(Nb,Ta)_6X_{12}$ -type clusters under any conditions (below). The dimensional parameters of the Zr–Z interactions (below) suggest these are at least comparable in strength to those present in binary Zr–Z phases, which are generally very refractory compounds. In contrast, the unoccupied niobium and tantalum halide clusters are held together by metal–metal bonding that is probably comparatively weak relative to that provided by the bridging halides, and all thermodynamically stable binary phases contain at least 15 cluster electrons.

Room Temperature Results. The well-known niobium and tantalum cluster examples that were just noted tolerate a lower electron count, i.e., 14, when the corresponding 15- or, more commonly, 16- e^- cluster is oxidized in solution near room temperature so that thermodynamic stability with respect to adjoining, condensed phases is not controlling.^{2,4,46} It appears that the same is true for centered zirconium clusters. The small list of 13-electron zirconium clusters found at high temperatures can be extended through analogous reactions in nonaqueous solvents, and in fact, a centered and distinctly larger 12-electron cluster example has been established as $Zr_6Cl_{18}Be^{4-}$.⁴⁷ The preparation of a possibly empty, 12-electron $Zr_6Cl_{12}(PMe_2Ph)_6$ by an undefined reaction process starting with $Zr_2Cl_6(PMe_2Ph)_4$ has recently been reported,⁴⁸ although exclusion of the 13-electron, hydrogen-centered counterpart does not appear possible with the information available. (The latter type is known in $Zr_6Cl_{12}H$, etc.^{8,9}) Their observed Zr–Zr distances are not particularly informative (below).

Interstitials, Cluster Dimensions, and Structure. The three dozen or so centered zirconium chloride cluster phases that have been characterized to date span 12 different structural types plus several variations thereon. Primary classification of these structures follows from their stoichiometries and the number of halides that must accordingly be shared between clusters in order to occupy all metal vertices. However, the means by which the prescribed number of cations, if any, are accommodated between the clusters in a compact structure are also important to the structure type, as in $Rb_5Zr_6Cl_{18}B$ (above). These possibilities have been particularly well demonstrated by the discovery of four distinctly different structure types (plus variations) for $(Zr_6Cl_{12}Z)Cl_{6/2}^{x-}$ networks which differ in "cluster ring" sizes and in the angles at bridging chlorine.^{10–13} The arrangement adopted in this group obviously depends on the number and size of the alkali-metal counterions that need to be incorporated and, to some degree, also on the size of Z. The rather poorly sized chlorine cavities utilized in some cases, as in Figure 3, give the impression that this is the least controlling feature.

The dimensions of the cation sites available between a particular arrangement of halogen-bridged clusters depend on a number of factors: the geometries of the intercluster linkages, the larger three-dimensional connectivity of the clusters, and the cluster size, and the last in turn depends on the effective size of a given interstitial, the magnitude of any intracenter matrix effect and, naturally, on the van der Waals radius of the halogen. A desire to be able to predict size trends and thence to gain some selectivity in the choice of structure type has led us to consider the reproducibility of and trends in interstitial size in zirconium chloride clusters. Figure 7 shows the Zr–Z distances (Å) determined by single-crystal means for 13 examples of 14-electron zirconium chloride clusters as a function of electrons on Z (H, Be–N).⁴⁹

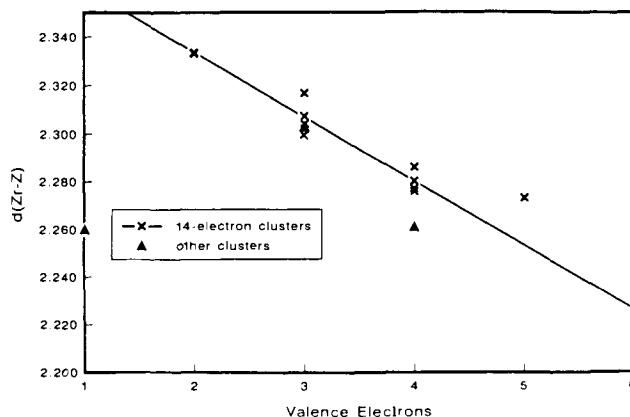


Figure 7. Average Zr–interstitial (Z) distances in structurally characterized $Zr_6Cl_{12}Z$ clusters⁴¹ plotted as a function of the number of valence electrons provided by first- and second-period interstitial elements. The line is the least-squares fit of the 14-electron cluster data (X) excluding $Zr_6Cl_{15}N$. The other examples (Δ) are $Cs_3Zr_6Cl_{16}C$ (15 e^-), $K_2Zr_6Cl_6Zr_6Cl_{12}H$, and $Li_6Zr_6Cl_{18}H$ (13 e^-).

These dimensions are seen to be remarkably consistent, although in a larger sense the behavior is not very surprising. The cluster dimensions, and therefore the Zr–Zr distances, seem to be determined almost exclusively by the Zr–Z contacts. This sort of matrix effect is analogous to the well-known fact that metal–metal separations in NaCl, CaF₂, etc. type structures are determined principally by metal–nonmetal separations.⁵⁰ As expected on the basis of covalent radii, Zr–Be distances are also longer than Zr–B distances, which are longer than Zr–C and Zr–N distances, and the trend appears linear at least from Be to C.

The operation of a cluster size effect in guiding a structure type selection is most apparent in the $Zr_6Cl_{15}Z$ family for larger Z, namely, for some larger beryllium-centered clusters^{7,12} and, especially, for those containing transition-metal interstitials like iron. In the latter instances, the intercluster bridges are both linear and shorter (smaller Cl^l–Cl^a matrix effect), and two interpenetrating cluster arrays are achieved in what is known as the Nb_6F_{15} structure. Only small cations like lithium can now be accommodated.¹³

Some interesting and informative deviations from the linear relationship are seen in Figure 7. Not surprisingly, the additional electron in the 15-electron $Cs_3Zr_6Cl_{16}C$ produces a shortening of the Zr–C separation of ~ 0.027 Å, but with the carbon "prop" the contraction is only about half that for the equivalent reduction in the $Nb_6Cl_{18}^{m-}$ series.⁴ On the other hand, removal of an electron from the optimal 14 in the formation of $Zr_6Cl_{14}B$ does not produce a significant lengthening [$\bar{d}(Zr–B) = 2.303$ Å⁹].

The larger than extrapolated value for Zr–N in $Zr_6Cl_{15}N$ is noteworthy and unexpected. Although cluster nitrides are relatively rare, a reasonable decrease of 0.041 Å in $\bar{d}(Sc–Z)$ for octahedral Z has been measured between the layered Sc_2Cl_2C and Sc_2Cl_2N .²⁹ A similar but less surprising radius anomaly occurs with the 13-electron clusters in $K_2Zr_6Cl_6Zr_6Cl_{12}H$ ³² and in $Li_6Zr_6Cl_{18}H$ ¹⁹ where $\bar{d}(Zr–H(\text{cluster centroid})) = 2.26$ Å in each (Figure 7). The latter distances well exceed normal Zr–H separations (≤ 2.10 Å), and the proton must be "rattling" in an oversized zirconium cluster, at least at room temperature.^{8,9} This cluster then must represent something like the minimum size for a zirconium chloride, with the $\bar{d}(Zr–Zr) = 3.20$ Å value largely determined by Zr–Zr (plus Zr–Cl^l and Cl^l–Cl^l) interactions alone. The onset of the same effect may be evidenced in the larger $Zr_6Cl_{15}N$ cluster as well. Examples with the smaller oxygen and fluorine interstitials are unknown. The size of the cluster in

(46) Fleming, P. D.; Dougherty, T. A.; McCarty, R. E. *J. Am. Chem. Soc.* **1967**, *89*, 159.

(47) Rogel, F.; Corbett, J. D., unpublished research.

(48) Cotton, F. A.; Kibala, P. A.; Roth, W. J. *J. Am. Chem. Soc.* **1988**, *110*, 299.

(49) The compounds represented in Figure 7 and the applicable references are: $K_2Zr_6Cl_6Zr_6Cl_{12}H$,²⁸ $Li_6Zr_6Cl_{18}H$,¹⁹ $KZr_6Cl_{15}Be$,⁷ $K_3Zr_6Cl_{15}Be$,¹² $Na_3Zr_6Cl_{15}Be$,¹⁴ $CsKZr_6Cl_{15}B$ (two independent values),¹⁰ $K_2Zr_6Cl_{15}B$,¹² $Ba_2Zr_6Cl_{17}B$,¹³ $Rb_5Zr_6Cl_{18}B$, this work; $Zr_6Cl_{14}C$,⁹ $Na_{0.5}Zr_6Cl_{15}C$,¹¹ $KZr_6Cl_{15}C$ (two values),¹⁰ $Zr_6Cl_{15}N$,¹¹ $Cs_3Zr_6Cl_{16}C$ (15 e^-).¹⁴ ($\sigma_d \leq 0.002$ Å except 0.008 Å for the next to the smallest $\bar{d}(Zr–B)$.)¹⁰

(50) Rundle, R. E. *Acta Crystallogr.* **1948**, *1*, 180.

$Zr_6Cl_{12}(PMe_2Ph)_6^{48}$ corresponds to $\bar{d}(Zr-Z) = 2.28 \text{ \AA}$. The influence of the terminal phosphine ligands on this is unclear (below), but the observed distance certainly does not preclude the presence of H.

Although the transferability of radii within most zirconium chloride clusters seems fairly good, secondary effects involving electron count, trans (terminal) ligands, and matrix effects must also be considered. Accordingly, the utility of such a system of radii in other systems may be only semiquantitative. The terminal ligand (halide) at each vertex is trans to the interstitial Z, and a less basic (lower charged) or more distant terminal ligand should result in a shortening of Zr-Z. This is the basis for the distortions observed in clusters that have different types of terminal halides, e.g., in Zr_6X_{14} , and the effect is probably of some importance with regard to the relatively short $\bar{d}(Zr-Z)$ values found in $Zr_6I_{12}Z$ clusters where all terminal halides are also edge-bridging in other clusters.²⁰ This behavior is in the opposite sense presumably responsible for a greater Zr-B separation found in $Rb_5Zr_6Cl_{18}B$, the largest value plotted at that ordinate in Figure 7, since all vertices now bind an unshared chloride. Nonetheless, the counter cations' interactions with the Cl^a must also be important, as seen by the fact that $Ba_2Zr_6Cl_{17}B$ provides the *smallest* value of $\bar{d}(Zr-B)$ shown, 2.300 Å.

The operation of a halide matrix effect based on halide size also appears in the few equivalent examples of zirconium iodide clusters that are available. In these cases, the Zr-Z distances are uniformly larger than in the chloride, i.e., by 0.053 Å in Zr_6I_4C , where the metal is nearly 0.5 Å inside the plane of the four neighboring Iⁱ atoms.

A more global approach to a system of possible standard radii for second-period interstitials shows deviations of the same order of magnitude. Nominal radii for carbon, nitrogen, etc. can be derived from the lattice dimensions of MC and MN phases in the rock salt structure with the aid of standard (and arbitrary but internally consistent) crystal radii.¹⁸ Thus, lattice dimensions for ZrC, HfC, NbC, and TaC on one hand and YN, ZrN, and NbN on the other yield six-coordinate, Zr-C and Zr-N bond distance predictions of 2.32 and 2.28 Å, respectively. These compare with ca. 2.28 Å for both in Figure 7, although only the carbon value can probably be taken very seriously. Experimental values for carbon close to those shown here can be similarly deduced from structural data for the condensed clusters in Y_4I_5C and $Sc_7Cl_{10}C_2$.⁵¹

The observed transferability of bond distances is in many respects rewarding and encouraging, supporting the notion that the carbon bonding in a $Zr_6Cl_{12}C$ -type cluster is not too different from that in ZrC even though the conventional band description for the latter²⁸ is much more difficult to translate into comparable terms. The contraction of $\sim 0.04 \text{ \AA}$ in the Zr-C distance seen on going from ZrC to the cluster may reflect primarily the replacement of the carbon on the zirconium "backside" by more polar bonds to chlorine. Solids are not that different from molecules in many respects. Notwithstanding, considerably greater *decreases* in Zr-Z distances on progressing from ZrZ_x binary phases to Zr_6Z -type clusters in polar intermetallics and then to $Zr_6I_{12}Z$ clusters, $\sim 0.15\text{--}0.25 \text{ \AA}$, have been recently noted with

Z = Si,²⁴ P,²⁶ Fe,⁵² etc. These changes parallel an increased oxidation state of zirconium, but more interpretational efforts are certainly needed in these instances.

Summary

The following features appear to be important regarding Zr_6X_{12} clusters and their relationship to those formed by niobium and tantalum:

1. A large family of cluster phases $A^1_x(Zr_6Cl_{12}Z)Cl_n$ can be systematically generated through selection of x , n and the encapsulated Z, which may be Be-N. No clusters are known that lack the centered Z element. Those with 14 cluster-based electrons are predominant.

2. The zirconium chloride cluster phases are distinctly different from the corresponding iodides. The iodides exhibit a much wider range of possible main-group Z elements and of cluster electron counts (13-16), but they occur in only two structure types, $Zr_6X_{12}Z$ and $(A^1)Zr_6X_{14}Z$.

3. MO calculations support the dominance of 14-electron clusters for the zirconium chlorides and demonstrate the importance of strong, polar Zr-Z bonding. Matrix effects associated with small Z, the larger iodine, or smaller niobium (and tantalum) atoms in M_6X_{12} clusters correlate well with the greater thermodynamic stability of the more reduced, 15- and 16-electron clusters in which the a_{2u} MO is occupied. This effect is thought to arise from diminished antibonding $M(xy)-X^i(\pi)$ contributions to the a_{2u} orbital of a M_6X_{12} cluster with increased cluster distortion because of a size disparity between X and M. The observation of less reduced niobium fluoride and oxide clusters is also consistent with this expectation.

4. The t_{2g}^6 HOMO for the centered 14-e⁻ clusters is only metal-metal bonding, but significant Zr-Zr overlap and bonding are also found in the interstitial-bonding a_{1g} and t_{2u} MOs, especially with the less electronegative interstitial elements.

5. The empty 15- or 16-electron $(Nb,Ta)_6X_{12}$ -type clusters are known to be reduced to 14-e⁻ examples only near room temperature. Twelve-electron examples of centered zirconium chloride clusters can be obtained under similar conditions.

6. Structure types exhibited by the $Zr_6Cl_{12}Z$ cluster family depend on the dimensions of both the cluster and the number and size of any cations. The interstitials Be, B, and C provide 14-e⁻ clusters with very reproducible dimensions that decrease in that order. On the other hand, encapsulated hydride and, evidently, nitride afford similar and apparently minimally sized units where other than Zr-Z bonding is determining.

Acknowledgment. This research was supported by the National Science Foundation, Solid-State Chemistry, via Grant DMR-8318616 and was carried out in facilities of the Ames Laboratory, DOE. R.P.Z. was also supported by Departmental Gilman and Procter and Gamble Fellowships.

Supplementary Material Available: Tables of anisotropic thermal parameters for $Rb_5Zr_6Cl_{18}B$ and parameters utilized in extended-Hückel calculations (3 pages); listing of observed and calculated structure factor data for $Rb_5Zr_6Cl_{18}B$ (5 pages). Ordering information is given on any current masthead page.

(51) Kauzlarich, S. M.; Hughbanks, T.; Corbett, J. D.; Klavins, P.; Shelton, R. N. *Inorg. Chem.* **1988**, *27*, 1791.

(52) Hughbanks, T.; Rosenthal, G.; Corbett, J. D. *J. Am. Chem. Soc.* **1988**, *110*, 1511.